



Universiteit  
Leiden  
The Netherlands

## **Roentgen stereophotogrammetric analysis to study dynamics and migration of stent grafts**

Koning, O.H.J.

### **Citation**

Koning, O. H. J. (2009, June 25). *Roentgen stereophotogrammetric analysis to study dynamics and migration of stent grafts*. Retrieved from <https://hdl.handle.net/1887/13870>

Version: Corrected Publisher's Version

License: [Licence agreement concerning inclusion of doctoral thesis in the Institutional Repository of the University of Leiden](#)

Downloaded from: <https://hdl.handle.net/1887/13870>

**Note:** To cite this publication please use the final published version (if applicable).

# CHAPTER

# 9

---

## **Fluoroscopic roentgen stereophotogrammetric analysis (FRSA) to study 3-D stent-graft dynamics in patients: a pilot study**

---

Olivier H. J. Koning  
Bart L. Kaptein  
Rozemarijn van der  
Vijver  
Nuno V. Dias  
Martin Malina  
Martin J. Schalijs  
Edward R. Valstar  
and J. Hajo van Bockel

*J Vasc Surg 2009; in press*

## Abstract

**Objective:** To study the feasibility and analyze the first results of Fluoroscopic Roentgen Stereophotogrammetric Analysis (FRSA) quantifying real time three-dimensional dynamic motion of stent-grafts (SG) in patients after endovascular aortic aneurysm repair (EVAR).

**Methods:** A digital bi-plane fluoroscopy set-up was calibrated (Siemens Axiom Artis dBc®). Stereo images were acquired of a patient after thoracic EVAR and of a patient after abdominal EVAR. Images were analyzed using a customized version of commercially available software for Roentgen stereophotogrammetric analysis (MB-RSA, MEDIS specials BV). SG motion was measured during the cardiac cycle with respiratory arrest. In addition, SG motion due to respiratory action was measured in the patient after abdominal EVAR.

**Results:** SG motion could be quantified in all 3 dimensions at 30 (stereo) frames per second in both patients without difficulty. For the thoracic SG, the maximum translational motions of the center of mass of the top stent in X-, Y-, and Z- direction (TM XYZ) were 2.3mm, 2.5mm, 1.9mm respectively. The diameter changed (DC) between 27.9mm and 28.7mm. Motion in axial direction (AX) was 2.9mm. Rotational motion around the longitudinal axis of the top stent (RM) was 3.5°. For the abdominal SG, the TM XYZ were 1.2mm, 1.0mm, 1.5mm respectively. DC: 22.8mm-23.5mm. AX: 1.6mm. RM: 1.1°. During respiratory action TM XYZ were 5.8mm, 1.5mm, 2.4mm respectively.

**Conclusion:** FRSA is the first validated clinically feasible tool to quantify real time three-dimensional stent-graft dynamics after EVAR. Because quantification of three-dimensional motion was not available until now, FRSA can provide crucial information of the continuous forces that are exerted in all directions on stent-grafts. Thus, it will provide essential information for further improvements in stent-graft design.

## Introduction

**E**ndovascular repair (EVAR) is widely accepted as a reliable technique for treatment of selected abdominal and thoracic aortic aneurysms. Stent-graft failure can occur due to the physically demanding environment in which the device is placed. The repetitive strain that is induced by the cardiac and respiratory cycle can result in device failure such as stent fractures, fabric perforation and migration. These failures are a threat to patient health and safety.<sup>1-3</sup> Detailed knowledge of stent-graft dynamics after EVAR is indispensable to minimize the risk of graft failure by continuously improving stent-graft design and testing.

Stent-graft dynamics appear to be complex and three-dimensional. Axial, transverse and rotational motion of the aorta, as well as dilatation have been reported to occur during the cardiac cycle.<sup>4-8</sup>

Currently, it is impossible to precisely quantify stent-graft dynamics with current clinically used imaging techniques. The two main modalities used to study stent-graft dynamics during the cardiac cycle are cinematographic (cine-) CT and MRI.<sup>4-6</sup> These techniques have several disadvantages and technical limitations. The most important of these is the fact that the reconstructions are limited to a single, two-dimensional plane.<sup>9</sup>

Recently, an experimental study was published on the use of fluoroscopic roentgen stereophotogrammetric analysis (FRSA) to quantify real time three-dimensional dynamics of stent-grafts during the cardiac cycle.<sup>10</sup> FRSA is a combination of a commercially available digital bi-plane fluoroscopic imaging system and the well known and validated method of roentgen stereophotogrammetric analysis, used to measure micromotion in-vivo.<sup>11-18</sup> FRSA uses calibrated, high resolution digital stereo images to assess the position of (metallic) markers using specialized software. The images are acquired at 30 stereo frames per second. The technique is completely non-invasive, does not require intravascular contrast and has a radiation exposure of approximately only 0.1 mSv for a 3 second study, which corresponds to 4 cardiac cycles at a heart rate of 80 bpm.<sup>10</sup>

In this study, we have evaluated the feasibility and obtained the first results of Fluoroscopic Roentgen Stereophotogrammetric Analysis (FRSA) to quantify real time three-dimensional dynamic motion of stent-grafts in patients after EVAR.

## Methods

### FRSA set-up

We used a Siemens Axiom Artis dBc imaging system (Siemens AG, Erlangen, Germany) (Figure 1), which consists of two C-arms with digital flat panel Roentgen detectors. The focus to detector distance was set at 95 cm. The two C-arms were positioned at a 90 degree angle, to produce a posterior-anterior image and a lateral image. The images were acquired and stored in 1024 x 1024 pixels, 14 bits grey scale resolution (Figure 2 and 3). The frame rate was 30 bi-directional images per second. Each stereo image was acquired as two separate alternating images, resulting in 60 alternating images per second. The set-up was calibrated to determine the exact relative position of the two Roentgen foci and the two detectors. The procedure was performed as described previously, using a calibration box with markers in known positions.<sup>10</sup> For each analysis reported in this study, a 1.5 second run (45 stereo images) was analyzed.



**Figure 1.** FRSA set-up consisting of two C-arms with digital flat panel Roentgen detectors (Siemens Axiom Artis dBc imaging system, Siemens AG, Erlangen, Germany).

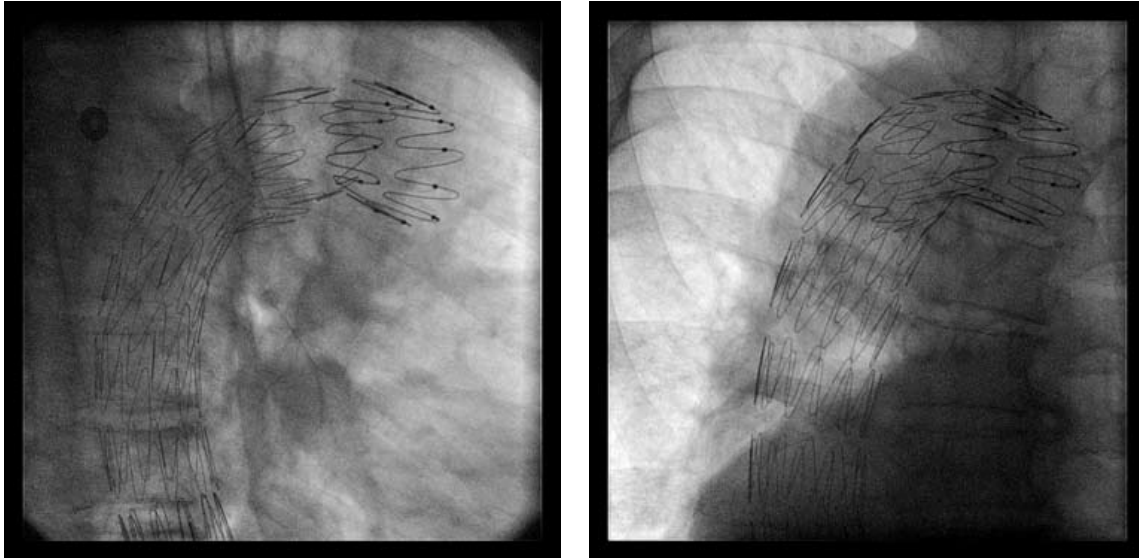


**Figure 2.** Lateral and Posterior-Anterior fluoroscopic images of the thoracic stent. The spherical shaped welding points and fabric markers are visible on the top stent.

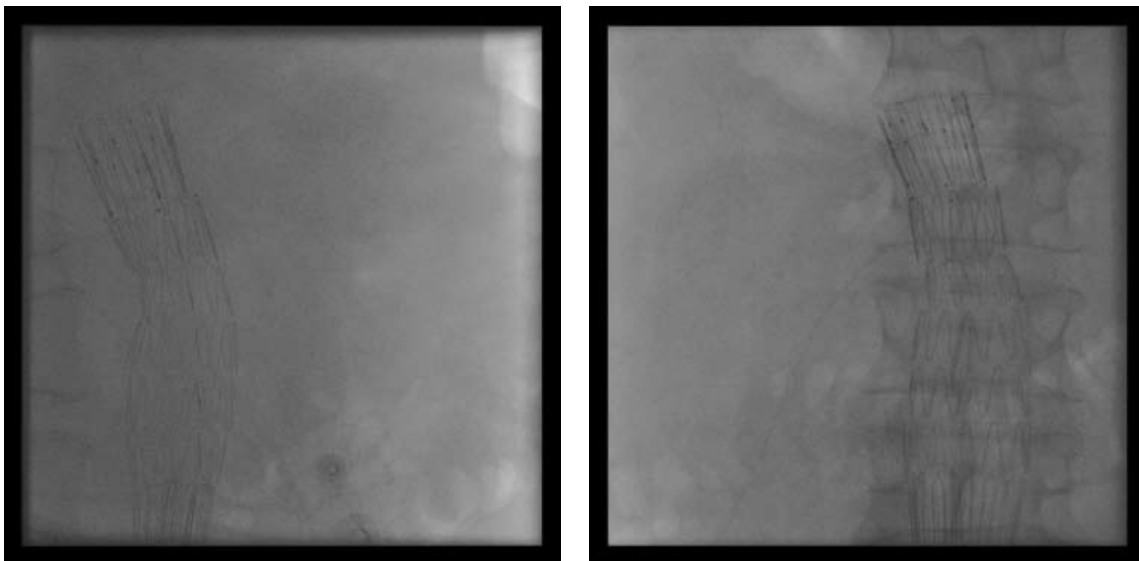


**Figure 3.** Lateral and Posterior-Anterior fluoroscopic images of the abdominal stent. The spherical shaped welding points and fabric markers are visible on the top stent.

The image pairs were analyzed using Model-based RSA software (ModelBased-RSA, version 3.2, MEDIS specials, Leiden, The Netherlands) to calculate the relative 3-D marker positions.<sup>10-16</sup> No image reconstruction is required before analyzing the image pairs.

### Patients

Two patients were randomly selected for this pilot study. Both had undergone EVAR within a week before evaluation. The first patient was a 57 year old male with a symptomatic type-B

aortic dissection.. A proximal component of a Zenith TX2® thoracic stent-graft device (Cook, Bjaeverskov, Denmark) was implanted, intentionally covering the ostium of the left subclavian artery. The graft had a diameter of 34mm. The blood pressure during imaging was 160/97 mmHg with a pulse rate of 100 per minute, which corresponds to 2.5 cardiac cycles during the 1.5 second image acquisition run. The imaging of the stent-graft dynamics during the cardiac cycle was performed during respiratory arrest.

The second patient was a 75 year old male with an abdominal aortic aneurysm. He was treated with a Zenith® stent-graft (Cook, Bjaeverskov, Denmark). The proximal graft diameter was 28mm. The patient had a blood pressure during imaging of 129/69 mmHg and a pulse rate of 80 per minute, which corresponds to 2 cardiac cycles during the 1.5 second image acquisition run. The imaging of the stent-graft dynamics during the cardiac cycle was performed during respiratory arrest. As an additional study, stent-graft displacement as a result of respiratory action was measured in a separate image run.

The study was approved by our institution's ethics review committee.

### **Analysis of stent-graft dynamics**

The welding points of the hooks to the top stent of the stent-graft were used as markers for 3D motion analysis, as well as the gold markers designating the upper edge of the fabric of the graft (Figure 4). The marker positions were determined in each sequential frame. The resulting series of marker positions was analyzed for marker motion. The changing position of the center of mass of the stent markers was used to quantify three-dimensional motion of the aorta – stent-graft complex during the cardiac cycle. Furthermore, a cylindrical shape was fitted through the cranial markers in every stereo image (12 markers for the thoracic stent and 11 markers for the abdominal stent). The changing diameter of the cylinders was used as a measure for the pulsatility of the stent. Finally, rotation and translation of the stent around and along the longitudinal stent axis were assessed. Analysis was performed using routines that were implemented in Matlab r2006B (The MathWorks, Natick, USA).

The origin of the coordinate system was placed in the center of the markers in the first image frame. The positive X-axis was oriented in caudal direction, the positive Y-axis in lateral direction towards the right side of the patient, and the Z-axis in dorsal direction.

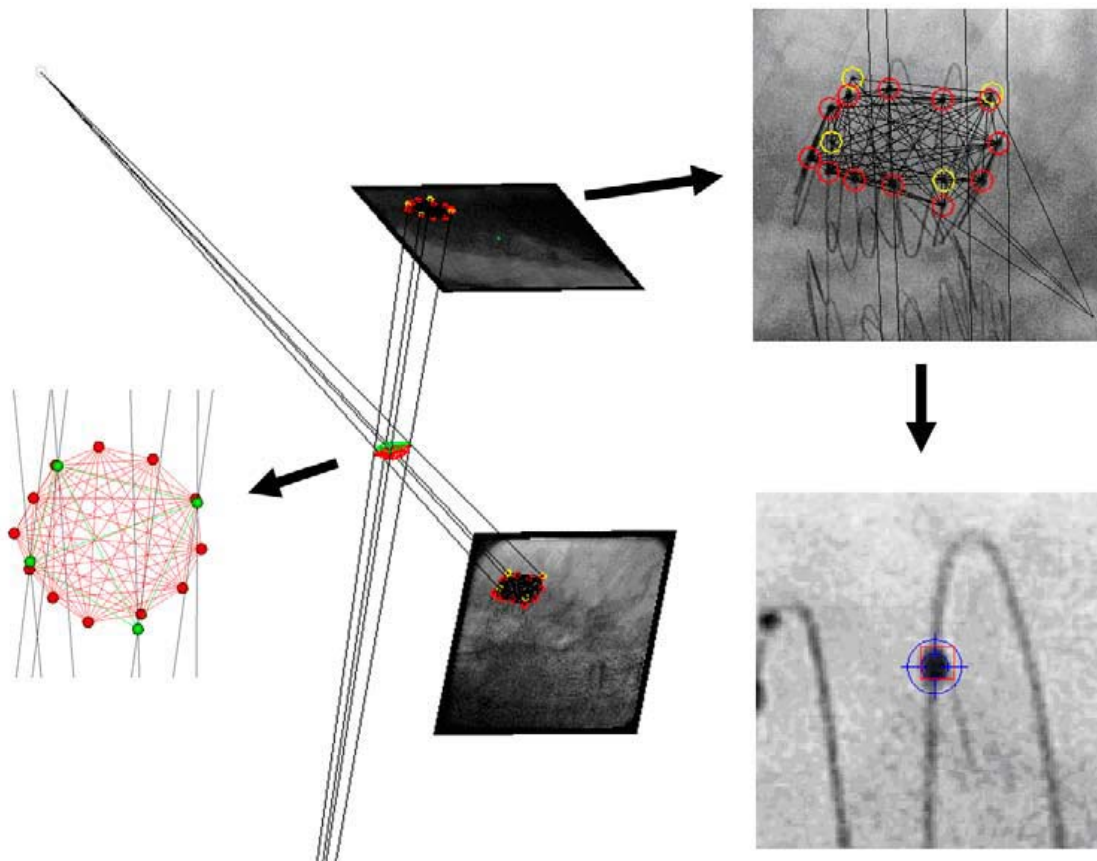


**Figure 4.** Overview of the stereo reconstruction of the thoracic stent-graft device. Center: 3D reconstruction of the stereo image and the Roentgen foci of the bi-plane set-up. The crossing lines reflect the position of the stent-graft markers. Left: Close-up of the 3D reconstructed markers, the red markers are reconstructed from the welding points of the hooks to the top-stent, and the green markers represent the gold markers at the upper edge of the fabric. Upper right: Close-up of the image with the detected markers, the red markers designate the welding points; the yellow markers designate the gold markers. Lower right: Close-up of a single welding point of the hook to the stent-graft. These welding points are used as markers to generate the 3D stent-graft image.

## Results

### Analysis of stent-graft dynamics

#### *Thoracic stent-graft*

Three-dimensional cyclic motion of the stent-graft was observed. Figure 2 shows the lateral and posterior-anterior images of a stereo image of the graft. Figure 4 shows a three-dimensional



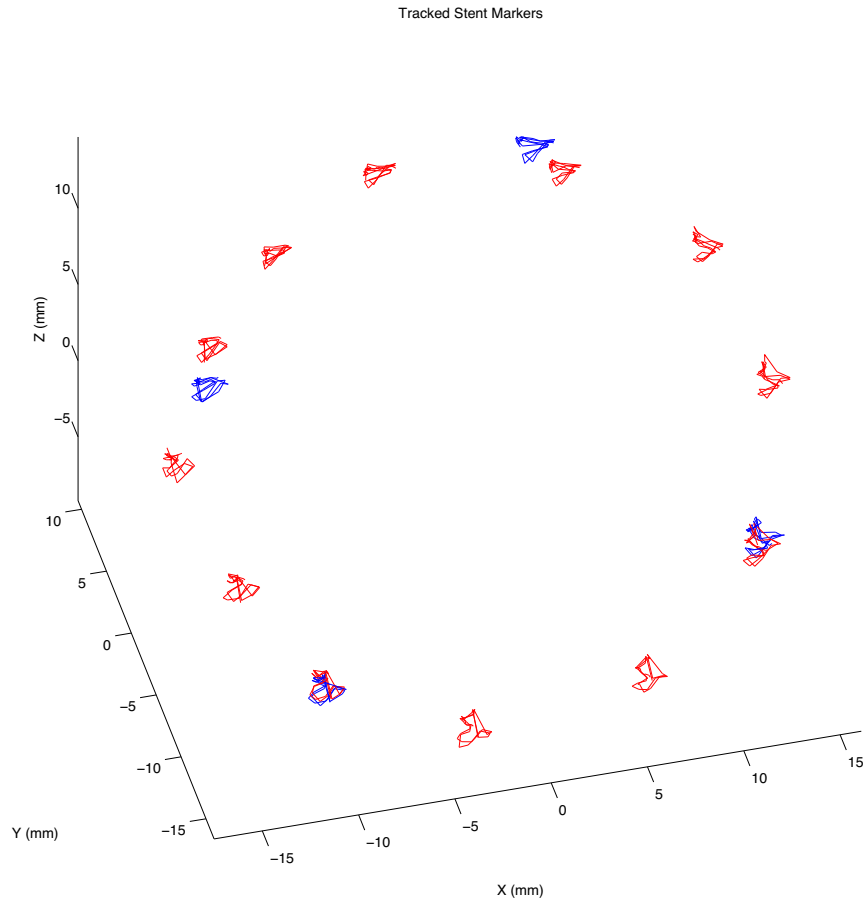


**Figure 5.** The tracked thoracic stent markers (welding points) (red) and gold fabric markers (blue).

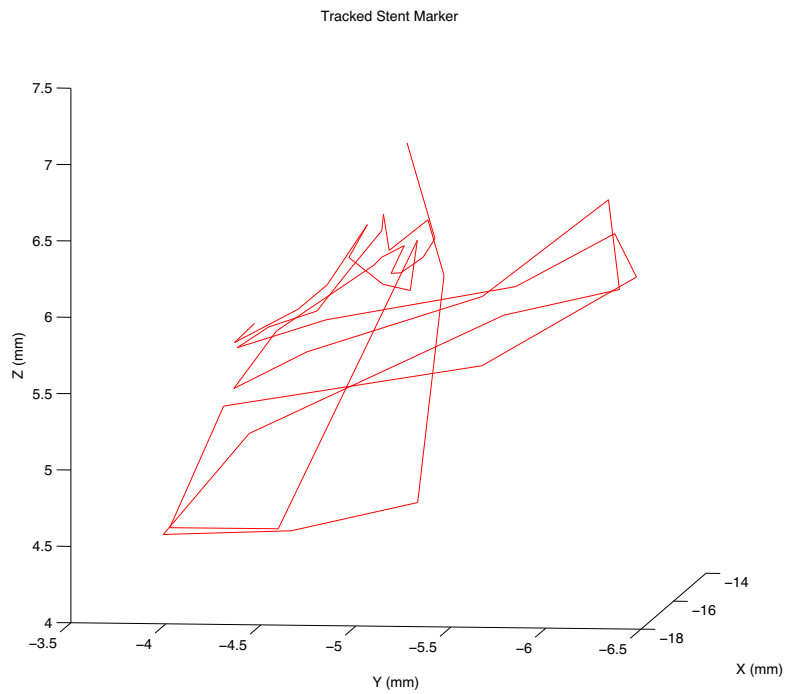


**Figure 6.** Detail of the typical track of a thoracic stent marker.

representation of the stent markers as reconstructed by the FRSA software. Figure 5 shows the position change of the stent markers and the gold fabric markers during the image acquisition run. Figure 6 shows the dynamics of a single, randomly chosen, marker during the cardiac cycle. Figure 7 shows a break down of all marker motions in X, Y and Z direction, relative to their positions at  $t=0.3$ , which is the start of the systole.

The dynamics of the center of mass of all markers are displayed in Figure 8, showing cyclic motion of the stent in all directions. The thoracic stent-graft showed a motion pattern of stent dilatation and a center of mass motion of the top stent in caudal-ventral-right hand side direction relative to the patient, followed by an over-compensation in opposite lateral and cranial direction and a gradual return to the starting position with reduction of diameter of the graft. This means that, at the start of the systole, the stent-graft moves toward the heart. This is probably due to contraction of the left ventricle. The maximum translational motions of the center of mass of the stent in X-, Y-, and Z- direction were 2.3mm, 2.5mm and 1.9mm respectively. A cylinder was fitted through the cranial markers of the stent-graft. The average distance from the markers to this cylinder was 0.14mm. The cyclic diameter change of the cylinder, between 27.9mm and 28.7mm, is also shown in Figure 8. The rotational motion of the top stent was  $3.5^\circ$  around its longitudinal axis. The stent motion along its long axis was 2.9mm per cycle.

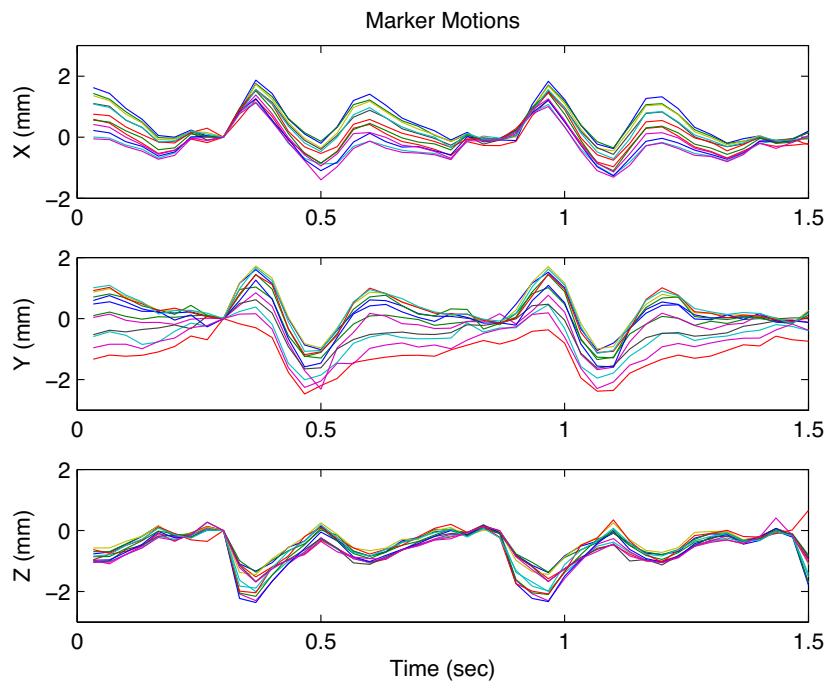


**Figure 7.** Motion of all thoracic stent markers relative to their first positions; break down in X, Y and Z direction. Note that the markers have different motion patterns as a result of the deformation of the stent.

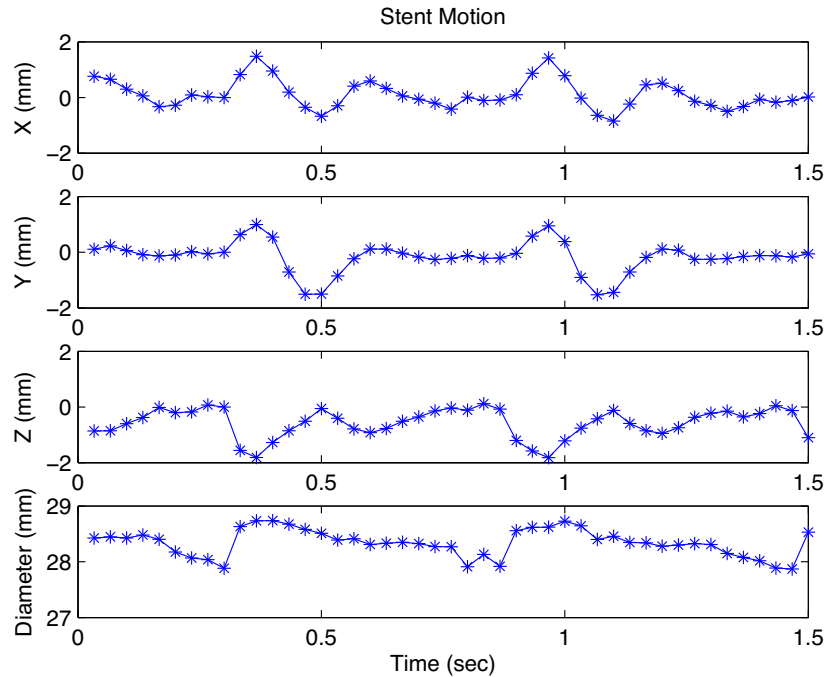


**Figure 8.** Thoracic stent motion (X, Y, Z motion of the center of mass of the top-stent and the change in diameter of the cylinder fitted through the stent markers).

### *Abdominal stent-graft*

Three-dimensional cyclic motion of the stent-graft was observed. Figure 3 shows the lateral and posterior-anterior images of a stereo image of the graft. Figure 9 shows the cyclic change of position of the center of mass of the top-stent. The maximum translational motions of the center of mass of the stent in X-, Y-, and Z-direction were 1.2mm, 1.0mm and 1.5mm respectively. The average distance from the markers to the cylinder that was fitted through the markers was 0.26mm. The diameter change of the cylinder was between 22.8mm and 23.5mm (Figure 9). The rotational motion of the top stent was  $1.1^\circ$  around its longitudinal axis. The stent motion along its long axis was 1.6mm per cycle.

As a result of respiratory action, the maximum translational motions of the top stent in X-, Y-, and Z-direction were 5.8mm, 1.5mm and 2.4mm respectively.

## Discussion

This study clearly demonstrates that fluoroscopic Roentgen stereophotogrammetric analysis (FRSA) is a clinically feasible, non-invasive tool to quantify real time 3-D stent-graft dynamics after EVAR in detail. For the first time, quantification of 3-D motion including rotational dynamics is possible.

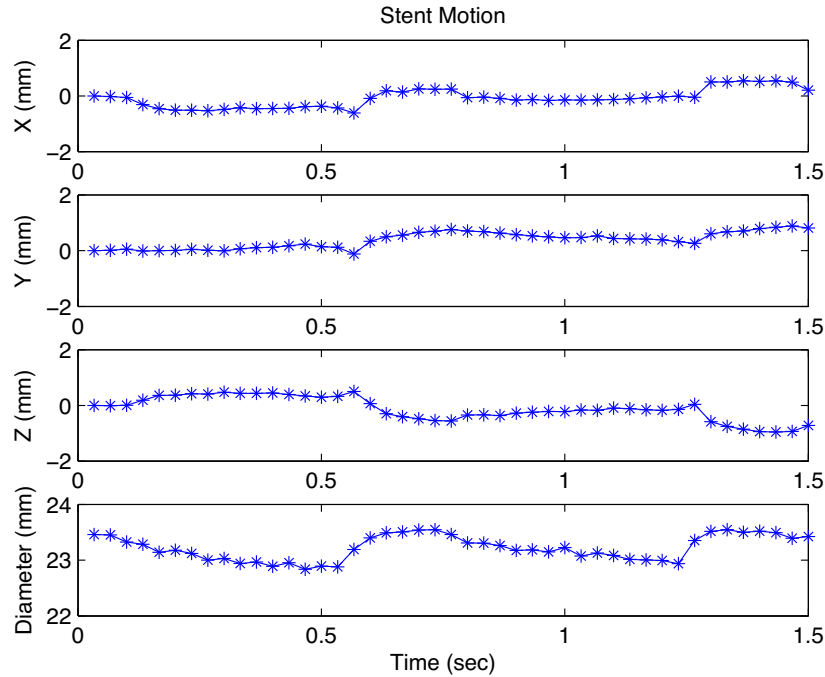


**Figure 9.** Abdominal stent motion (X, Y, Z motion of the center of mass of the top-stent and the change in diameter of the cylinder fitted through the stent markers).

Previous experimental validation studies have shown that the fast stereo image acquisition and high frame rate of FRSA enable accurate and precise quantification of stent-graft motion in high spatial and temporal resolution, with a mean measurement error of  $0.003 \pm 0.019$  millimeter.<sup>10</sup>

Image acquisition itself is painless, of short duration, does not require intravascular contrast and with a radiation exposure of 0.1 mSv the patient burden is very low.

The clinical data found in this study are limited in size. Therefore, it is of little interest to extensively discuss the nature and implications of the stent-graft motion found in these two patients. However, to point out the possible implications of our findings, it is interesting to review part of the presented data. The thoracic stent-graft showed a three-dimensional motion pattern of stent dilatation and a center of mass motion. If the dynamics of this thoracic stent-graft are assessed in a single reconstruction plane, as is the case with cine-CT or cine-MRI, the initial segment of the aorta as viewed in the first reconstructed image would be out of the reconstruction plane almost all the time. Only at the end of the diastole will it return to the initial position in the image reconstruction plane. As a result of this out of plane motion, dynamics of conically shaped stent-grafts or change of stent-graft angulation during cyclic motion can result in false measurements of shape or diameter change. Therefore, FRSA is much more powerful than

current cinematographic imaging using cine-CT and cine-MRI as it enables quantification of the true changes of three-dimensional stent-graft position and configuration.

We found a significant motion of the abdominal stent-graft due to respiratory action of almost 6mm in caudal direction. When using plain abdominal radiography to detect long-term stent-graft migration, the dynamics due to respiratory action could result in under- or over-reporting of migration in individual cases. This is due to the change of position of the stent-graft as compared to the reference point, the vertebral column.

The results demonstrate that standard markers used for positioning of the graft during EVAR can easily be used for FRSA, as well as welding points of the hooks to the top stent. As an alternative to marker detection, automated pattern recognition of the stent-graft could be used to facilitate measurements without the need for markers. These aspects of FRSA are subject to further evaluation at our institutions. In contrast to standard Roentgen stereophotogrammetric analysis used to detect graft migration during long term follow-up with comparison of multiple investigations over time<sup>12,17,18</sup>, additional markers in the wall of the aorta are not required to perform these dynamic measurements.

Contrary to cine-CT and cine-MRI, there are no limitations to FRSA in terms of direction of motion, type of motion or type of metal of the stent-graft, duration of image acquisition or ECG changes. Furthermore, no intravascular contrast is required. Motion analysis with cine-CT and cine-MRI is limited to a single (2-Dimensional) plane due to the reconstruction of the images.<sup>9</sup> Out-of-plane motion can not be quantified and complex three-dimensional motion can only be interpreted semi-quantitatively by analyzing different image planes. Moreover, rotational motion can not be quantified at all. In addition, the spatial resolution of these techniques is limited<sup>6</sup> and their accuracy and reproducibility have not been validated. Because FRSA uses direct three-dimensional reconstruction of the images, the listed limitations do not apply to this technique. Another disadvantage of cine-CT and -MRI is that both require intravascular contrast. Difficulties with ECG reconstruction, as is required with these techniques, can occur in patients without sinus rhythm. The resulting CT or MRI image is a compilation of several cardiac cycles, resulting in a "time average" dynamic image, rather than an actual "real time" view of the stent-graft motion. Contrary to cine-CT and -MRI, FRSA does not require ECG reconstruction because it uses real time images to quantify three-dimensional motion. Therefore, there are no technical time constraints or difficulties with ECG abnormalities with this technique. Finally, there are inherent technique specific disadvantages such as a high radiation dose in cine-CT and the limitations in imaging stainless steel stent-grafts in cine-MRI.

There are still many unknown aspects of stent-graft motion in-vivo. The cardiac and respiratory cycle, in conjunction with tissue properties of the aortic wall and surrounding tissues, result in repetitive strain on the stent-graft. This strain has led to stent-graft failure resulting in devastating complications, despite intensive testing before clinical introduction.<sup>1,2</sup> The main reason for this kind of device failure is that preclinical testing depends on modeling of motion and forces acting on the stent-graft. Unexpected types of stent-graft motion, including stent-graft torsion, have revealed unanticipated forces acting on the stent-graft. These forces could obviously not have been modeled beforehand and therefore device failure was not anticipated.

Detailed knowledge of stent-graft motion after EVAR is vital to stent-graft development and improvement. Only with this knowledge it is possible to optimize modeling of graft safety testing and improve design e.g. by improved biocompatibility and (computer aided) fatigue modeling and bench testing. FRSA enables this kind of detailed real time imaging. Furthermore, modeling can be adjusted with the information obtained with FRSA after implantation in patients.

One could argue that assessment of the dynamics of a new stent-graft should be mandatory in the period of first clinical introduction to possibly detect unexpected motion in an early phase to determine if adequate bench testing has been performed and predict possible failure by fatigue modeling according to clinical motion data.

Currently, the only limitations of FRSA are that the field of view is limited by the detector size and that specifically identifiable markers are required to detect stent-graft position in consecutive images. We could visualize up to 8 stents of the thoracic or abdominal graft in one view (Figure 2 and 3) with the standard size digital detectors used for cardiac imaging. Larger detectors are commercially available and could enable imaging of the full length of longer grafts.

We plan to expand FRSA imaging and motion analysis to different stent-grafts and larger cohorts, as well as repeated imaging over time to study changes in motion pattern. The relative position change of the different stents of the stent-graft can also be measured. This way, angulation change and stent-graft torsion can be determined.

## Conclusion

FRSA is the first clinically feasible tool to quantify real time three-dimensional stent-graft dynamics after EVAR. Because quantification of three-dimensional motion was not available until now, FRSA can provide crucial information of the continuous forces that are exerted in all directions on stent-grafts. Thus, it will provide essential information for further improvements in stent-graft design.

## Acknowledgements

We would like to acknowledge the help of the following persons:

J.F. Hamming MD, PhD and J.W. Hinnen, MD, PhD, Department of Surgery, and E.H. Garling, Department of Orthopedics, Leiden University Medical Center, for their help with the study and critical review of the manuscript.

M. Boonekamp, Department of Fine Mechanics, LUMC, for his assistance in building the calibration object.

J. Geleijns, MSc, PhD and P.W. de Bruin, MSc, PhD, Clinical Physics, Department of Radiology, for their work on radiation dose measurement of FRSA.

## References

1. Bockler D, von Tengg-Kobligk H, Schumacher H, Ockert S, Schwarzbach M, Allenberg JR. Late surgical conversion after thoracic endograft failure due to fracture of the longitudinal support wire. *J Endovasc Ther.* 2005 Feb;12(1):98-102.
2. Jacobs TS, Won J, Gravereaux EC, Faries PL, Morrissey N, Teodorescu VJ, et al. Mechanical failure of prosthetic human implants: a 10-year experience with aortic stent graft devices. *J Vasc Surg.* 2003 Jan;37(1):16-26.
3. Tiesenhausen K, Hessinger M, Konstantiniuk P, Tomka M, Baumann A, Thalhammer M, Portugaller H. Surgical conversion of abdominal aortic stent-grafts--outcome and technical considerations. *Eur J Vasc Endovasc Surg.* 2006 Jan;31(1):36-41.
4. Verhagen, HJ, Teutelink A, Olree M, Rutten A, de Vos AM, Raaijmakers R, et al. Dynamic CTA for cutting edge AAA imaging: Insights into aortic distensibility and movement with possible consequences for endograft sizing and stentdesign *J Endovasc Ther.* 2005;12:1-45.
5. Teutelink A, Rutten A, Muhs BE, Olree M, van Herwaarden JA, de Vos AM, et al. Pilot study of dynamic cine CT angiography for the evaluation of abdominal aortic aneurysms: implications for endograft treatment. *J Endovasc Ther.* 2006 Apr;13(2):139-44.
6. Vos AW, Wisselink W, Marcus JT, Vahl AC, Manoliu RA, Rauwerda JA. Cine MRI assessment of aortic aneurysm dynamics before and after endovascular repair. *J Endovasc Ther* 2003;10:433-9.
7. Teutelink A, Muhs BE, Vincken KL, Bartels LW, Cornelissen SA, van Herwaarden JA, Prokop M, Moll FL, Verhagen HJ. Use of dynamic computed tomography to evaluate pre- and postoperative aortic changes in AAA patients undergoing endovascular aneurysm repair. *J Endovasc Ther.* 2007 Feb;14(1):44-9.
8. Flora HS, Woodhouse N, Robson S, Adiseshiah M. Micromovements at the aortic aneurysm neck measured during open surgery with close-range photogrammetry: implications for aortic endografts. *J Endovasc Ther.* 2001;8:511-520.
9. Muhs BE, Vincken KL, Teutelink A, Verhoeven EL, Prokop M, Moll FL, Verhagen HJ. Dynamic cine-computed tomography angiography imaging of standard and fenestrated endografts: differing effects on renal artery motion. *Vasc Endovascular Surg.* 2008 Feb-Mar;42(1):25-31.
10. Koning OH, Kaptein BL, Garling EH, Hinnen JW, Hamming JF, Valstar ER, Bockel JH. Assessment of three-dimensional stent-graft dynamics by using fluoroscopic roentgenographic stereophotogrammetric analysis. *J Vasc Surg.* 2007 Oct;46(4):773-779.
11. Selvik G. Roentgen stereophotogrammetry. A method for the study of the kinematics of the skeletal system. *Acta Orthop Scand Suppl.* 1989;232:1-51.
12. Karrholm J. Roentgen stereophotogrammetry. Review of orthopedic applications. *Acta Orthop Scand.* 1989;60:491-503.
13. Valstar ER, Vrooman HA, Toksvig-Larsen S, Ryd L, Nelissen RG. Digital automated RSA compared to manually operated RSA. *J Biomech.* 2000;33:1593-1599.
14. Vrooman HA, Valstar ER, Brand GJ, Admiraal DR, Rozing PM, Reiber JH. Fast and accurate automated measurements in digitized stereophotogrammetric radiographs. *J Biomech.* 1998;31:491-498.
15. Valstar ER, de Jong FW, Vrooman HA, Rozing PM, Reiber JH. Model-based Roentgen stereophotogrammetry of orthopaedic implants. *J Biomech.* 2001;34:715-722.
16. Kaptein BL, Valstar ER, Stoel BC, Rozing PM, Reiber JAC. A new model-based RSA method validated using CAD models and models from reversed engineering. *J Biomech.* 2003;36:873-882.
17. Koning OH, Oudegeest OR, Valstar ER, Garling EH, van der Linden E, Hinnen JW, et al. Roentgen Stereophotogrammetric Analysis: an accurate tool to assess endovascular stentgraft migration. *J Endovasc Ther.* 2006;13:468-475
18. Koning OH, Garling EH, Hinnen JW, Kroft LJ, van der Linden E, Hamming JF, et al. Accurate detection of stentgraft migration in a pulsatile aorta using Roentgen Stereophotogrammetric Analysis. *J Endovasc Ther.* 2007;14(1):30-8.



